



# Virtual monochromatic reconstructions of dual energy CT in abdominal trauma: optimization of energy level improves pancreas laceration conspicuity and diagnostic confidence

Gavin Sugrue<sup>1</sup> · John P. Walsh<sup>1</sup> · Yilin Zhang<sup>1</sup> · Bonnie Niu<sup>1</sup> · Francesco Macri<sup>1</sup> · Elina Khasanova<sup>1</sup> · Omar Metwally<sup>1</sup> · Nicolas Murray<sup>1</sup> · Savvas Nicolaou<sup>1</sup>

Received: 31 March 2020 / Accepted: 13 May 2020 / Published online: 30 May 2020  
© American Society of Emergency Radiology 2020

## Abstract

**Purpose** Pancreatic injury is associated with significant morbidity and mortality. Pancreatic lacerations can be challenging to identify as the pancreas is not scanned at peak enhancement in most trauma CT protocols. This study qualitatively and quantitatively assessed pancreatic lacerations with virtual monoenergetic dual-energy CT (DE CT) to establish an optimal energy level for visualization of pancreatic lacerations.

**Methods** Institutional review board approval was obtained. We retrospectively examined 17 contrast-enhanced CT studies in patients with blunt trauma with MRCP, ERCP, or surgically proven pancreatic lacerations. All studies were performed in our Emergency Department from 2016 to 2019 with a 128 slice dual-source DE CT scanner. Conventional 120 kVp and noise-optimized virtual monoenergetic imaging (VMI) datasets were created. VMI energy levels were constructed from 40 to 100 keV in 10 keV increments and analyzed quantitatively and qualitatively. Pancreatic laceration attenuation, background parenchymal attenuation, and noise were calculated. Qualitative assessment was performed by two independent readers.

**Results** The optimal CNR for the assessment of pancreatic lacerations was observed at VMI-40 in comparison with standard reconstructions and the remaining VMI energy levels ( $p = 0.001$ ). Readers reported improved contrast resolution, diagnostic confidence, and laceration conspicuity at VMI at 40 keV ( $p = 0.016$ ,  $p = 0.002$ , and  $p = 0.0012$  respectively). However, diagnostic acceptability and subjective noise were improved on conventional polyenergetic images ( $p = 0.0006$  and  $p = 0.001$  respectively).

**Conclusion** Dual energy CT at VMI-40 maximizes the CNR of pancreatic laceration, improves diagnostic confidence, and increases laceration conspicuity.

**Keywords** Dual energy computed tomography · Pancreas · Trauma

---

✉ Gavin Sugrue  
g\_sugrue@hotmail.com

John P. Walsh  
john.walsh@vch.ca

Yilin Zhang  
yilin.zhang95@gmail.com

Bonnie Niu  
bonnie.niu@vancouverimaging.com

Francesco Macri  
francesco.macri@yahoo.it

Elina Khasanova  
khasanovamd@yahoo.com

Omar Metwally  
Omar.Metwally@vch.ca

Nicolas Murray  
nicolas.murray.2@gmail.com

Savvas Nicolaou  
Savvas.Nicolaou@vch.ca

<sup>1</sup> Department of Emergency and Trauma Radiology, Vancouver General Hospital, University of British Columbia, Vancouver, BC V5Z 1M9, Canada

## Introduction

Blunt pancreatic trauma is an uncommon injury [1] and is associated with significant morbidity and mortality [2] due to non-specific clinical and laboratory findings [3] and failure or delayed diagnosis of a pancreatic injury. Prompt and accurate diagnosis of a pancreatic injury is made more challenging as the pancreas is often not scanned at peak enhancement (35–45 s) in most trauma CT protocols [4].

Evaluation of the abdomen with multidetector CT has long been accepted and validated as the reference standard in the acute setting [5]. Advances in DE CT post-processing algorithms [6], including bone marrow edema, iodine overlay maps, renal and gallstone analysis, has led to its increasing clinical use. Utilizing DE CT, images can be constructed to simulate the appearance of images obtained using a pure monoenergetic X-ray source, termed virtual monoenergetic imaging (VMI). VMI uses a complex post-processing algorithm on dual-energy datasets to construct “monoenergetic” energy levels [7, 8] expressed in kiloelectron volts (keV). VMI at low keV levels maximizes the conspicuity of iodine as it closely approximates the k-edge of iodine (33 keV) [9]. Consequently, VMI has demonstrated benefit in oncologic [10–12] and vascular [13] imaging. In the setting of trauma, VMI at lower energy levels improves the CNR of hepatic and splenic lacerations [14]; however, visualization of pancreatic lacerations using VMI has not yet been assessed. Thus, the purpose of this study is to qualitatively and quantitatively assess pancreatic lacerations to establish an optimal virtual monoenergetic energy level for visualization of pancreatic lacerations.

## Material and methods

### Study population

Institutional review board approval was obtained. We retrospectively examined 17 contrast-enhanced CT studies in patients with blunt trauma with MRCP, ERCP, or surgically proven pancreatic lacerations. All studies were performed in the Emergency Department of a Level 1 trauma centre from January 2016 to May 2019 using a standardized CT protocol on a dual-source dual-energy CT scanner. Patients who were not scanned using dual energy did not receive iodinated intravenous contrast, and those who did not have MRCP, ERCP, or surgically proven pancreatic injuries were excluded from the study.

### CT acquisition

CT images were acquired using a third-generation (Somatom Definition Force, Siemens Healthcare, Forchheim Germany)

dual-source dual energy 128-slice multirow detector CT system. The portal venous DE CT abdomen and pelvis, which was used for analysis in this study, is acquired 70 s post injection of 80 ml of intravenous contrast (Omnipaque 350 mg I/ml; GE Healthcare, USA) at a rate of 2.5 cc per second followed by 30 cc of 0.9% NaCl at the same rate. The CT abdomen is acquired with a low-pitch (pitch = 0.6) helical acquisition with tube voltages of 90 kV and 150 kV with Tin filter (mAs 115 and 89, respectively) with a rotation time of 0.5 s. At the scanner, DECT raw data were automatically reconstructed using the standard linear-blending technique by applying a blending factor of 0.6 (M<sub>0.6</sub>; 60% of the 90-kV and 40% of the 150-kV spectrum). Standard linearly blended reconstructions were obtained to simulate conventional 120-kV single-energy image acquisition. Axial source data were reconstructed with sinogram-affirmed iterative reconstruction algorithm (ADMIRE Siemens Healthcare, Forchheim, Germany) using a strength of 2.

### Image post-processing

DE CT raw data was post-processed on a 3D multimodality workstation (Syngo.via, version VB20, Siemens Healthcare, Forchheim, Germany) using a soft tissue (I30) convolution kernel (Qr40, Siemens). Virtual monoenergetic data sets were subsequently generated at 40 to 100 keV in 10 keV increments using the monoenergetic plus (Mono+) algorithm (Syngo.via, version VB20, Siemens Healthineers) (Fig. 1). Energy levels greater than 100 keV were not generated as they demonstrate significantly reduced iodine levels. Each VMI energy level data set and the conventional mixed dataset were reconstructed in axial and coronal slices with a thickness and increment of 3 mm respectively. Data sets were transmitted to a DICOM workstation (Osirix v10.0), to allow free-hand regions of interests (ROI) to be drawn and ROI copy-and-paste function.

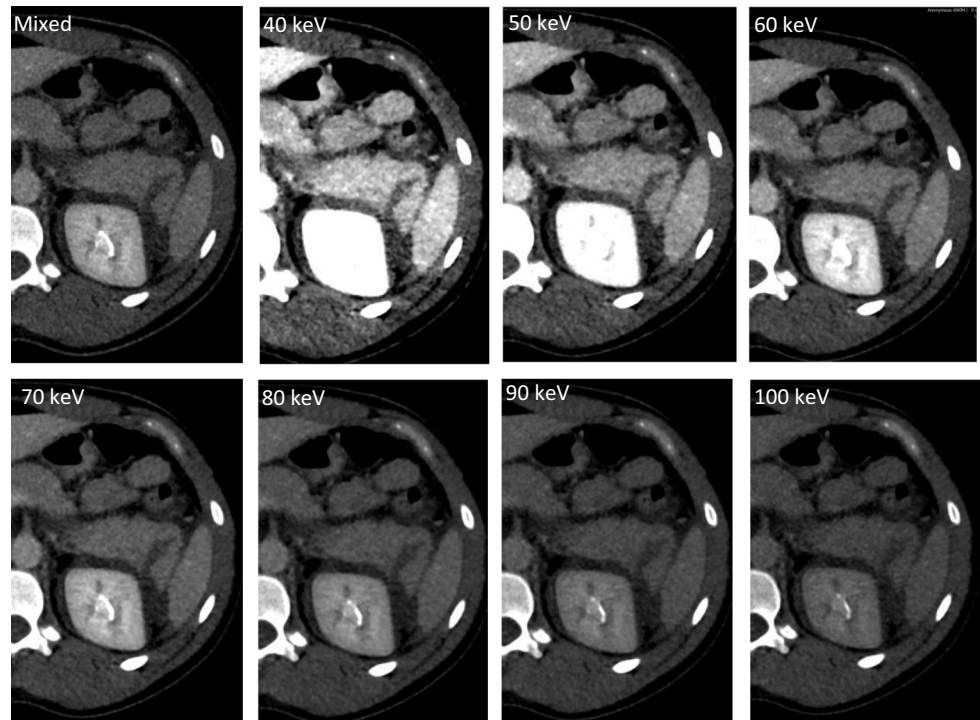
### Effective dose measurements

Dose length product (DLP) was documented from the dose report for each patient. The effective dose was calculated by multiplying the DLP by 0.015 mSv/mGy cm [15].

### Quantitative image analysis

Quantitative analysis of the conventional and virtual monoenergetic data sets was performed on the portal venous phase using Osirix by a radiologist with 5-year experience. A laceration was defined as a hypoenhancing region of pancreatic tissue compared to normally enhancing parenchyma. Firstly, the HU of the pancreatic laceration was calculated using the free-hand ROI tool (Fig. 2). The largest ROI as possible was drawn (> 100 mm<sup>2</sup>). Measurements were performed three times and averaged to ensure consistency and

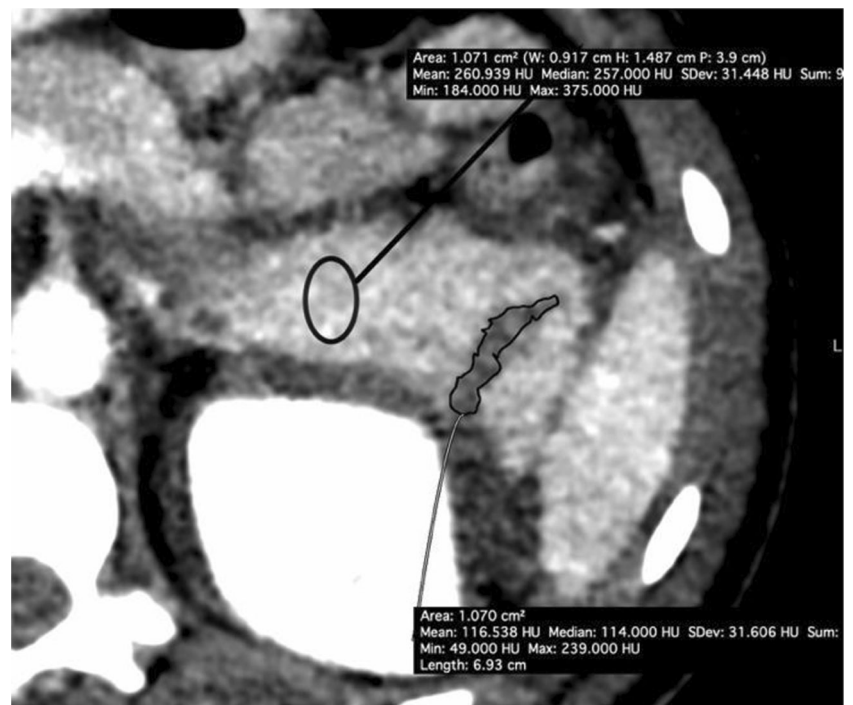
**Fig. 1** A 25-year-old male with a laceration through the tail of the pancreas illustrated on conventional and VMI energy levels from 40 to 100 keV. All images have the same display window (360HU) and same level (160 HU) settings



minimize inaccuracies. Secondly, ROIs were placed within the normal pancreas to calculate mean attenuation (HU) and noise (standard deviation of the mean attenuation) of the normal pancreas. Efforts were made to place the ROIs in an as homogeneous area as possible. Using the copy-and-paste function, the same sized ROI in the same location was maintained across all eight data sets (mixed, 40, 50, 60, 70, 80, 90,

100 keVs). Injury-to-parenchyma contrast was calculated using the following equation:  $HU_{organ} - HU_{injury}$ . For calculating the injury-to-parenchyma contrast-to-noise ratio (CNR), the following formula was used:  $CNR = (HU_{organ} - HU_{injury}) / SD_{organ}$ . The SD is the mean background noise of normal pancreas [16].

**Fig. 2** A 25-year-old male with a laceration the tail of the pancreas. Illustration of the ROIs used to calculate HU of the pancreatic laceration, normal pancreatic parenchyma and noise of the organ



## Qualitative image analysis

Based on the results of the qualitative analysis, two radiologists with 8 and 15 years' experience independently assessed the VMI-40 and conventional mixed sets. Readers were aware that all patients had a pancreatic laceration, and were blinded to VMI energy level. Readers were allowed to modify the default window settings (width, 400 HU; level, 100 HU), as the optimal window settings vary significantly depending on the VMI energy level [17]. Image quality was assessed using parameters adapted from prior studies [10, 18]. Diagnostic acceptability was scored out of 3 with 1 = standard and diagnostic, 2 = acceptable and diagnostic only after windowing, and 3 = perceptible change that affects interpretation. Subjective noise was graded out of 3, with 1 = standard and diagnostic, 2 = noisy but diagnostic, and 3 = noisy and non-diagnostic. Contrast resolution was graded out of 3, where 1 = excellent, 2 = acceptable, and 3 = poor. Diagnostic confidence was graded out of 3, where 1 = confident, 2 = somewhat confident, and 3 = not confident. Subjective conspicuity of all visible lesions was graded on a four-point scale adapted from a prior study [19], with 1 = the laceration is strikingly evident and easily detected, 2 = definite laceration detected, 3 = subtle finding but likely a laceration, and 4 = barely perceptible laceration with presence debatable.

## Statistical analysis

Statistical analysis was performed with SPSS (version 25; IBM, Armonk, NY). Pancreatic laceration CNR at the conventional mixed and seven different VMI energy levels (40–100 keV) were compared using a one-way ANOVA with Tukey post test. Comparison between the qualitative parameters of image quality was performed using a paired *T* test. A *p* value of <0.05 was considered statistically significant. All data was presented as mean  $\pm$  standard deviation.

## Results

We included 17 consecutive patients (mean age 37, range 16–64 years) including 10 males and 7 females. Further, 16/17 patients sustained blunt abdominal trauma. Ten pancreatic lacerations were located in the tail of the pancreas, five within the body, and two within the head of pancreas. By imaging modality, ten patients were diagnosed on DE CT (58.8%) without further diagnostic imaging evaluation prior to surgery. Five (29.4%) patients underwent a MRI and two (11.8%) underwent ERCP after initial evaluation with DE CT to confirm the presence of a pancreatic injury.

## Effective dose measurements

The average DLP was 329.5 mGy cm ( $\pm$  146.9 mGy.cm) and the effective dose was 4.94 mSv ( $\pm$  2.2 mSv).

## Quantitative image analysis

### Noise

Noise was significantly higher at 40 keV compared to noise at other virtual monoenergetic levels and conventional images ( $p < 0.001$ ) (Table 1, Fig. 3) Noise was lowest at 100 keV (11.4). A similar noise level was observed at 90 keV and conventional mixed images (11.8 for 90 keV and 11.9 for mixed ( $p = 0.98$ ) (Table 1, Fig. 3).

### Injury-to-normal parenchyma contrast

The HU attenuation of the pancreatic laceration to normal pancreatic parenchyma was higher at lower monoenergetic levels, with the highest attenuation at 40 keV ( $p < 0.001$ ) (Table 1, Fig. 3). Higher injury-to-normal pancreas contrast ratios were observed at lower energy levels (40, 50, 60, 70) compared with conventional images ( $p = 0.04$ ). Further, 80 keV provided an equivalent injury-to-normal parenchyma ratio compared to conventional images (69.2 for 80 keV and 69.0 for conventional ( $p = 0.90$ ) (Table 1, Fig. 3).

### Contrast to noise

Lower VMI energy levels demonstrated an increased injury-to-parenchyma CNR (Table 1, Fig. 3). The highest CNR was at 40 keV, significantly higher than conventional images (6.6 for 40 keV, 5.0 for conventional,  $p = 0.001$ ). CNR at 40, 50, 60 were higher compared with conventional images (6.6, 6.2, 5.8, and 5.0 respectively). CNR at 70 keV was equivalent to conventional images, 5.0 and 5.0 respectively ( $p = 0.98$ ) (Table 1, Fig. 3).

## Qualitative image analysis

At the VMI 40 energy level, both readers observed improved contrast, diagnostic acceptability, and confidence compared to conventional mixed images. Conventional images showed significantly improved diagnostic acceptability and subjective noise (Table 2). Two of the ten pancreatic lacerations were only identified on the VMI-40 datasets, and were not detected on conventional 120 kVp mixed images.

**Table 1** Mean pancreatic laceration-to-pancrehyma contrast, background noise of the normal pancreatic parenchyma, and laceration contrast-to-noise ratio (CNR) for conventional images and VMI (virtual monoenergetic imaging)

Energy level	Laceration contrast	Pancreas noise	CNR	CNR <i>p</i> value*
Conventional	69.0 ± 23.2	11.9 ± 4.5	5.0 ± 2.1	–
40 keV	217.8 ± 73.5	33.4 ± 7.6	6.6 ± 2.8	< 0.001
50 keV	151 ± 49.1	24.2 ± 6.1	6.2 ± 2.7	< 0.001
60 keV	110.4 ± 38.2	18.3 ± 5.1	5.8 ± 2.9	0.04
70 keV	86.3 ± 23.6	15.2 ± 4.5	5.0 ± 2.3	0.95
80 keV	69.2 ± 21.7	12.8 ± 3.9	4.8 ± 2.4	0.32
90 keV	58.2 ± 18.4	11.8 ± 3.1	3.9 ± 1.9	< 0.001
100 keV	50.7 ± 19.9	11.4 ± 3.1	3.4 ± 1.7	< 0.001

\* *p* values were calculated by comparing each virtual monoenergetic series with the conventional images using a paired *t* test. A value of *p* < 0.05 was considered significant

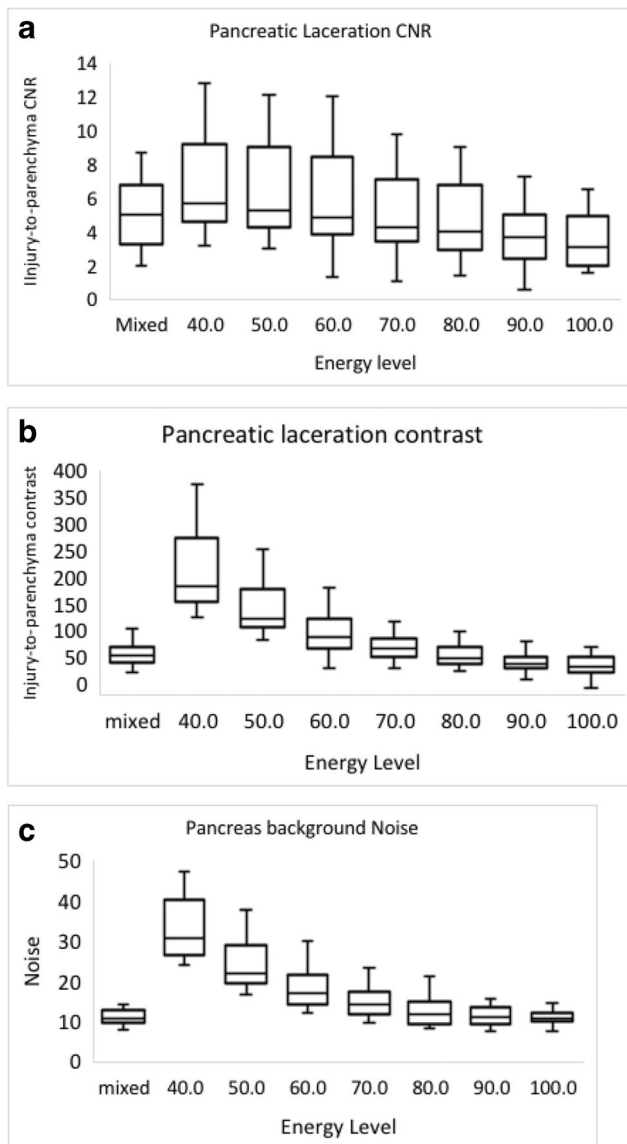


**Fig. 3** Quantitative parameters across the virtual monoenergetic energy levels (40–100 keV) reconstructed from contrast-enhanced dual energy abdomen CT data. For pancreatic laceration ROIs, the optimal CNR, and laceration contrast occurred at 40 keV (a, b). Maximal noise occurred at 40 keV (c)

## Discussion

The presence of a pancreatic laceration has a significant impact on determining patient management and prognosis. Thus, accurate identification and classification of a laceration allows for timely intervention. Our findings demonstrate that despite an increase in image noise, low-energy VMI improves quantitative and qualitative image parameters in patients with pancreatic lacerations compared to conventional linearly blended M<sub>0.6</sub> image series. Therefore, we recommend that low-energy VMI energy levels be routinely reconstructed when performing DE CT of the abdomen in the setting of trauma.

Solid-organ lacerations are characterized by hypoenhancing regions compared to normally enhancing parenchyma. Identification of regions of pancreatic hypoenhancement can be challenging as the pancreas is not routinely scanned at optimal pancreatic enhancement as part of the trauma CT abdomen and pelvis protocol (pancreatic parenchymal phase 20 s vs. portal venous phase 70 s). As illustrated in our study, the pancreatic laceration CNR is higher at lower energy levels (VMI 40–60) compared to conventional mixed images, resulting in improved diagnostic confidence and laceration conspicuity. The improved CNR

**Table 2** Comparison of subjective imaging parameters between conventional (120 kVp) and VMI-40 kVp datasets. Diagnostic acceptability, subjective noise, contrast resolution, and confidence were graded on a three-point system. Conspicuity was graded on a four-point system. Data are mean ± standard deviation

Parameter	VMI-40	Conventional	<i>p</i> value
Diagnostic acceptability	1.9 ± 0.49	1.2 ± 0.33	0.0006
Subjective noise	1.9 ± 0.49	1.3 ± 0.47	0.001
Contrast resolution	1.3 ± 0.47	1.8 ± 0.56	0.0156
Confidence	1.1 ± 0.33	1.7 ± 0.47	0.002
Conspicuity	1.1 ± 0.33	1.7 ± 0.47	0.0012

VMI virtual monoenergetic imaging

at lower VMI energy levels is due to lower energy levels more closely approximate the k-edge of iodine. Consequently, there is an increase in the conspicuity of the iodine content, thus increasing the contrast between a region of hypoenhancement (i.e., a laceration) and uninjured pancreatic parenchyma. In particular, we noted that VMI-40 best delineated the laceration, demonstrating maximal CNR and injury-to-normal pancreas contrast. This finding is in keeping with other oncological studies demonstrating that lower VMI levels (ranging from 50 to 60 keV) [20–23] improve lesion detection by increasing CNR.

Our study is the first to report on the utility of DE CT in the assessment of pancreatic lacerations, and is consistent with a study [14] illustrating that 40 keV is the optimal energy level for assessing both splenic and liver lacerations. Given the high probability of concomitant visceral injuries (90%) in the setting of pancreatic trauma [24], our study adds to the growing evidence illustrating the benefit of reconstructing lower VMI energy levels in the setting of trauma.

Significant advances in the VMI algorithm, termed VMI+ as used in our study, now allows for high image contrast at lower VMI energy levels with improved noise reduction [25]. Despite an increase in image noise and reduction in diagnostic acceptability of the images (table) at lower VMI energy levels, VMI-40 images are still diagnostically acceptable and improve diagnostic confidence. This finding is consistent with other studies [13, 14, 22]. Thus, we recommend VMI images be interpreted in conjunction with conventional mixed images. Radiologists interpreting VMI images should be aware that due to an increase in contrast at lower energy levels [26], a more significant adjustment of the window level and width adjustment may be required.

Limitations of this study include the single institution retrospective nature of the study. In addition, the study population is small ( $n = 17$ ), part of which reflects the low incidence of pancreatic lacerations. Thirdly, the quantitative and qualitative analysis was based on a direct comparison between the standard linearly blended M<sub>0.6</sub> image series and the VMI+ algorithm. Other blending factors (for example M<sub>0.3</sub> or M<sub>0.5</sub>) and other VMI energy levels (i.e., 50–100 keV) were not analyzed and would be of interest in further studies. Further, the study was performed using a dual-source dual-energy CT scanner (third-generation Somatom Definition FORCE, Siemens) and the Siemen's VMI+ algorithm. Our findings are vendor and manufacture specific and may be not be generalizable to other DE CT products. Finally, prior to image assessment, readers were aware that all patients had surgical, ERCP, or MRCP proven pancreatic lacerations which may have had an impact on the readers diagnostic confidence.

In conclusion, contrast-enhanced dual source dual energy CT at VMI-40 maximizes the CNR of a pancreatic laceration, improves diagnostic confidence, and increases laceration

conspicuity. We recommend the routine reconstruction of 40-keV VMI images as part of the trauma DE CT abdomen protocol.

**Authors' contributions** Conceptualization: Gavin Sugrue and John Walsh. Methodology: Gavin Sugrue, John Walsh Yilin Zhang, and Bonnie Niu. Formal analysis and investigation: Gavin Sugrue, John Walsh Omar Metwally, and Francesco Macri. Writing—original draft preparation: Gavin Sugrue and Elina Khasanova. Writing—review and editing: Gavin Sugrue, John Walsh, and Omar Metwally. Supervision: Savvas Nicolaou and Nicolas Murray.

## Compliance with ethical standards

**Conflict of interest** Dr. Savvas Nicolaou: Research grant, Siemens.

**Availability of data and material** All our data and materials as well as software application or custom code support our published claims and comply with field standards.

**Code availability (software application or custom code)** Not applicable.

**Authors disclosures** Gavin Sugrue, MD: none; John Walsh, MD: none; Yilin Zhang: none; Bonnie Niu, BSc: none; Francesco Macri, MD: none; Elina Khasanova, MD: none; Omar Metwally, MD: none; Nicolas Murray, MD: none; Savvas Nicolaou, MD: Institutional research grant from Siemens Healthineers.

**Ethical approval** Institutional review board approved the study.

## References

- Daly KP, Ho CP, Persson DL et al (2008) Traumatic retroperitoneal injuries: review of multidetector CT findings. *Radiographics* 28: 1571–1590
- Stawicki SP, Schwab CW (2008) Pancreatic trauma: demographics, diagnosis, and management. *Am Surg* 74:1133–1145
- Lin BC, Chen RJ, Fang JF et al (2004) Management of blunt major pancreatic injury. *J Trauma Acute Care Surg* 56:774–778
- Goshima S, Kanematsu M, Kondo H et al (2006) Pancreas: optimal scan delay for contrast-enhanced multi-detector row CT. *Radiology* 241:167–174
- Paolantonio P, Rengo M, Ferrari R et al (2016) Multidetector CT in emergency radiology: acute and generalized non-traumatic abdominal pain. *Br J Radiol* 89:20150859
- Murray N, Darras KE, Walstra F et al (2019) Dual-energy CT in evaluation of the acute abdomen. *RadioGraphics* 39:264–286
- Marin D, Nelson RC, Schindera ST et al (2009) Low-tube-voltage, high-tube-current multidetector abdominal CT: improved image quality and decreased radiation dose with adaptive statistical iterative reconstruction algorithm—initial clinical experience. *Radiology* 254:145–153
- Silva AC, Morse BG, Hara AK et al (2011) Dual-energy (spectral) CT: applications in abdominal imaging. *Radiographics* 31:1031–1050
- Yu L, Christner JA, Leng S et al (2011) Virtual monochromatic imaging in dual-source dual-energy CT: radiation dose and image quality. *Med Phys* 38:6371–6379
- Darras KE, Clark SJ, Kang H et al (2019) Virtual monoenergetic reconstruction of contrast-enhanced CT scans of the abdomen and

- pelvis at 40 keV improves the detection of peritoneal metastatic deposits. *Abdom Radiol* 15(44):422–428
11. Wang Q, Shi G, Qi X et al (2014) Quantitative analysis of the dual-energy CT virtual spectral curve for focal liver lesions: characterization. *Eur J Radiol* 83:1759–1764
  12. Hou WS, Wu HW, Yin Y et al (2015) Differentiation of lung cancers from inflammatory masses with dual-energy spectral CT imaging. *Acad Radiol* 22:337–344
  13. Albrecht MH, Scholtz JE, Husers K et al (2016) Advanced image-based virtual monoenergetic dual-energy CT angiography of the abdomen: optimization of kiloelectron volt settings to improve image contrast. *Eur Radiol* 26:1863–1870
  14. Sun EX, Wortman JR, Uyeda JW et al (2019) Virtual monoenergetic dual-energy CT for evaluation of hepatic and splenic lacerations. *Emerg Radiol* 8:1–7
  15. Huda W, Ogden KM, Khorasani MR (2008) Converting dose length product to effective dose at CT. *Radiology* 248:995–1003
  16. Yamada Y, Jinzaki M, Hosokawa T et al (2014) Abdominal CT: an intra-individual comparison between virtual monochromatic spectral and polychromatic 120-kVp images obtained during the same examination. *Eur J Radiol* 83:1715–1722
  17. De Cecco CN, Caruso D, Schoepf UJ et al (2016) Optimization of window settings for virtual monoenergetic imaging in dual-energy CT of the liver: a multi-reader evaluation of standard monoenergetic and advanced imaged-based monoenergetic datasets. *Eur J Radiol* 85:695–699
  18. Darras KE, McLaughlin PD, Kang H et al (2016) Virtual monoenergetic reconstruction of contrast-enhanced dual energy CT at 70 keV maximizes mural enhancement in acute small bowel obstruction. *Eur J Radiol* 85:950–956
  19. Shuman WP, Green DE, Busey JM et al (2014) Dual-energy liver CT: effect of monochromatic imaging on lesion detection, conspicuity, and contrast-to-noise ratio of hypervascular lesions on late arterial phase. *Am J Roentgenol* 203:601–606
  20. Martin SS, Pfeifer S, Wichmann JL et al (2017) Noise-optimized virtual monoenergetic dual-energy computed tomography: optimization of kiloelectron volt settings in patients with gastrointestinal stromal tumors. *Abdom Radiol* 42:718–726
  21. Martin SS, Wichmann JL, Weyer H et al (2017) Dual-energy computed tomography in patients with cutaneous malignant melanoma: comparison of noise-optimized and traditional virtual monoenergetic imaging. *Eur J Radiol* 95:1–8
  22. De Cecco CN, Caruso D, Schoepf UJ et al (2018) A noise-optimized virtual monoenergetic reconstruction algorithm improves the diagnostic accuracy of late hepatic arterial phase dual-energy CT for the detection of hypervascular liver lesions. *Eur Radiol* 28:3393–3404
  23. Lenga L, Czwilka R, Wichmann JL et al (2018) Dual-energy CT in patients with colorectal cancer: improved assessment of hypoattenuating liver metastases using noise-optimized virtual monoenergetic imaging. *Eur J Radiol* 106:184–191
  24. Reki S, Anderson SW, Rhea JT et al (2010) Imaging of blunt pancreatic trauma. *Emerg Radiol* 17:13
  25. Grant KL, Flohr TG, Krauss B et al (2014) Assessment of an advanced image-based technique to calculate virtual monoenergetic computed tomographic images from a dual-energy examination to improve contrast-to-noise ratio in examinations using iodinated contrast media. *Investig Radiol* 49:586–592
  26. Fu W, Marin D, Ramirez-Giraldo JC, Choudhury KR et al (2017) Optimizing window settings for improved presentation of virtual monoenergetic images in dual-energy computed tomography. *Med Phys* 44(11):5686–5696

**Publisher's note** Springer Nature remains neutral with regard to jurisdictional claims in published maps and institutional affiliations.